

Short communication

Porous silicon biosensor for detection of viruses

Andrea M. Rossi^{a,b,c,*}, Lili Wang^b, Vytas Reipa^b, Thomas E. Murphy^a

^a Department of Electrical and Computer Engineering, University of Maryland, College Park, MD 20742, USA

^b Biochemical Science Division, National Institute of Standards and Technology, 100 Bureau Drive, Stop 8312, Gaithersburg, MD 20899, USA

^c Nanotechnology Department, Istituto Nazionale di Ricerca Metrologica, Strada delle cacce, 91 10135 Torino, Italy

Received 15 February 2007; received in revised form 26 May 2007; accepted 8 June 2007

Available online 21 July 2007

Abstract

There is a growing need for virus sensors with improved sensitivity and dynamic range, for applications including disease diagnosis, pharmaceutical research, agriculture and homeland security. We report here a new method for improving the sensitivity for detection of the bacteriophage virus MS2 using thin films of nanoporous silicon. Porous silicon is an easily fabricated material that has extremely high surface area to volume ratio, making it an ideal platform for surface based sensors. We have developed and evaluated two different methods for covalent bioconjugation of antibodies inside of porous silicon films, and we show that the pore penetration and binding efficiency depend on the wettability of the porous surface. The resulting films were used to selectively capture dye-labeled MS2 viruses from solution, and a viral concentration as low as 2×10^7 plaque-forming units per mL (pfu/mL) was detectable by measuring the fluorescence from the exposed porous silicon film. The system exhibits sensitivity and dynamic range similar to the Luminex liquid array-based assay while outperforming protein micro-array methods. © 2007 Elsevier B.V. All rights reserved.

Keywords: Porous silicon; Biosensor; Fluorescence; MS2; Antibody; Bioconjugation

1. Introduction

Nanometer-scale features are observed in a variety of biological systems, and have evolved to enable a diverse array of functionality. These systems have motivated the development of synthetic, engineered nanoscale systems that could potentially mimic or augment these biological systems. It is therefore important to study the functionalization of such nanoscale materials and their subsequent interaction with biomolecules of comparable dimension. One application that can clearly take advantage of nanometer-scale structures is biosensors. For sensor applications, nanoscale materials provide a large and often highly reactive surface area, which enables more effective capture and detection of molecules than bulk materials. We describe here a new ultrasensitive technique that uses nanoporous silicon to measure small quantities of the bacteriophage virus MS2.

Porous silicon (PS) (Uhlir, 1956) was first developed in the 1950s and exhibits unique optical and electrical properties due to quantum confinement effects (Canham, 1990; Cullis et al., 1997). Porous silicon is easily produced by electrochemical etching in a solution of hydrofluoric (HF) acid, and the pore diameter can be controllably varied from a few nanometers up to several hundred nanometers by adjusting the etching parameters (Herino et al., 1987; DeStefano et al., 2004). After electrochemical etching, the internal pore surfaces of the porous silicon are hydrogen-terminated, which allows one to immobilize large quantities of biomolecules in a relatively small volume through bioconjugation (Mathew and Alocilja, 2005). Consequently, PS can serve as a versatile platform for a biosensor with optical or electrical detection. Silicon is often a material of choice in nanobiodevice design (Borini et al., 2005) as it is biocompatible and readily susceptible to chemical surface derivatization (Buriak, 2002). Here we present our results in developing a prototype fluorescence-based virus sensor using nanoporous silicon.

Viruses are smaller than bacteria and present considerable challenges for detection (Wick and McCubbin, 1999). The bacteriophage virus MS2 was chosen as a model analyte that is often used for simulating biological warfare agents. It is a 27 nm RNA virus that infects *Escherichia coli* male (Stockley et al., 1994).

* Corresponding author at: Department of Electrical and Computer Engineering, University of Maryland, College Park, MD 20742, USA.
Tel.: +1 301 975 8605.

E-mail address: amrossi@umd.edu (A.M. Rossi).

We have successfully conjugated a rabbit anti-MS2 antibody inside the PS film using two covalent conjugation protocols. The antibody binding strength and porous layer penetration measurements show that maintaining surface hydrophilicity is critical in achieving high protein concentrations inside the porous material. The sensor selectivity and dynamic range were evaluated using fluorescence measurements with dye labeled bacteriophage MS2 virus. The sensor was shown to be capable of detecting virus concentrations as low as 2×10^7 plaque-forming units per mL (pfu/mL), with three orders of magnitude of dynamic range.

2. Materials and methods

2.1. Porous film preparation

The porous silicon films were prepared using pulsed anodic etching in an HF electrolyte solution (Föll, 1991). The electrolyte solution was held in a cylindrical PVC electrochemical cell, with a platinum sheet as a cathode and a polished p-doped crystalline silicon wafer as the anode ((1 0 0) boron doped, $\rho = 0.5\text{--}1.0\text{ m}\Omega\text{ cm}$, Virginia Semiconductor, VA).¹ The wafer was gently pressed against cell opening through a 1.3 cm diameter Viton O-ring that limited the etched area to 1.32 cm². The etching solution was comprised of three parts hydrofluoric acid (48%, J.T. Baker, Phillipsburg, PA) and one part of anhydrous ethanol. Etching was performed using a sequence of current pulses, supplied by a programmable galvanostat (Princeton Applied Research, Model 273A). Each pulse applied a current density of 300 mA/cm² to the silicon for a duration of 200 ms, followed by a 10 s pause to allow for equilibration of the HF concentration and the removal of hydrogen bubbles that form inside of the pores during etching.

Porous silicon layers were etched to a depth of either 100 or 1000 nm, by using two different etching times. The porous film thickness was determined by selectively removing the porous layer in a solution of potassium hydroxide and measuring the resulting step-height with a profilometer.

After forming the porous layers, the chips were rinsed in deionized water and ethanol and subsequently blown dry with N₂ gas. Fig. 1 presents a top-down and cross-sectional scanning-electron micrograph of a representative porous film, showing an average pore dimension of 50 nm.

2.2. Bioconjugation chemistry

The electrochemical etching and drying procedure described above results in a porous silicon film in which the internal surfaces are hydrogen terminated (Cullis et al., 1997; Bensliman et al., 2004). Bioconjugation of the porous silicon is accomplished by replacing the hydrogen with a functional organic group that

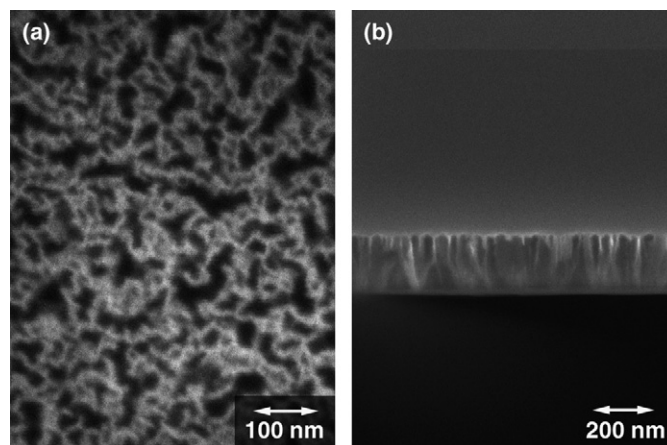


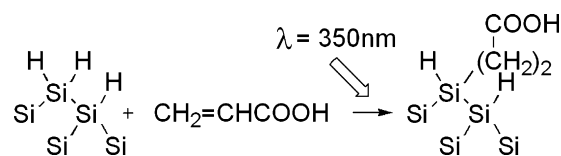
Fig. 1. (a) Top-down and (b) cross-sectional scanning electron micrographs of the porous silicon films produced by electrochemical etching.

can be bound to the desired protein molecule using a cross-linker. We have tested two procedures to make a covalent bond between the rabbit MS2 antibody and the porous silicon surface, one using carbodiimide based protein conjugation and the other based on TDBA-OSu, a photoactivatable aryldiazirine cross-linker. Both procedures have been used in the past for protein immobilization on silicon surfaces (Wang et al., 2004).

For the carboxyl group immobilization the porous silicon sample was put in a quartz cuvette in contact with a 10% volume solution of monomeric acrylic acid in ethanol. The solution was deaerated by means of oxygen-free N₂ flux to prevent the photo-generated radical reaction inhibition and was then exposed to 350 nm light for 1 h in a UV reactor (RMR600, Southern New England Ultraviolet Company, Branford, CT) under continuous nitrogen flux. The silicon samples were then thoroughly washed in ethanol and dried under nitrogen flux. This procedure replaces the silicon surface hydrogen termination with carboxyl terminated functionalities, according to Scheme 1.

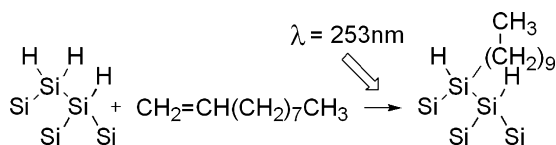
The acrylic acid-derivatized porous silicon surface was next immersed in a 0.02 M MES (2-[*N*-morpholino]ethane sulfonic acid) buffer solution (pH 4.8) containing either Alexa 488-labeled or un-labeled anti-MS2 antibodies (0.15 mg/mL), to which 12 μ L of 1-ethyl-3-[3-dimethylaminopropyl] carbodiimide hydrochloride (EDC) solution in deionized water (10 mg/mL) was added. This reaction was carried out in the dark with gentle mixing for 2 h, followed by rinsing in DI water and nitrogen drying.

For the second functionalization method, an aryldiazirine cross-linker is inserted into the C–H bonds of the methylene groups within the hydrocarbon chain through a highly reactive carbene intermediate (Wang et al., 2004). First, the methylene groups were made available by grafting a hydrocarbon



Scheme 1.

¹ Certain commercial equipment, instruments, materials, or companies are identified in this paper to specify adequately the experimental procedure. In no case does such identification imply recommendation or endorsement by the National Institute of Standards and Technology, nor does it imply that the materials or equipment identified are the best available for the purpose.



Scheme 2.

chain using a photo-assisted silicon reaction in the alkene solution (Buriak, 2002). The porous silicon sample was immersed in a quartz cuvette, containing deaerated decene and exposed to 253 nm light for 2 h using the photo-reactor, according to Scheme 2.

Next, a diazirine/succinimidyl bilinker was used to bind the anti-MS2 antibody to the methyl terminated PS surface. The alkylated Si surface was activated via a cross-linker, 4-benzoylbenzoic acid (BBA), succinimidyl ester in deaerated anhydrous carbon tetrachloride using a quartz micro-cell under 365 nm UV light illumination for 15 min. After the cross-linking reaction, the activated porous silicon surface was washed with carbon tetrachloride and immediately immersed in a solution containing Alexa 488 dye-labeled rabbit anti-MS2 antibodies.

2.3. Fluorophore labeling of antibody and virus

The rabbit anti-MS2 antibodies in phosphate-buffered saline (PBS) and MS2 viruses in PBS/1.5 mM MgCl₂ went through buffer exchange to 0.1 M sodium carbonate buffer, pH 8.3, by using Pro Spin columns from Princeton Separations Inc. (Adelphia, NJ). The conjugation of either Alexa 488 to the antibodies or Alexa 532 fluorophores to MS2 viruses was carried out according to the manufacturer-recommended procedure. The same spin columns were used for separation of the antibodies and MS2 viruses from free fluorophores and buffer exchange to PBS, pH 7.2, 0.05% sodium azide for labeled antibodies and PBS, pH 7.2, 0.05% sodium azide, 1.5 mM MgCl₂ for labeled MS2 viruses. The fluorophore per antibody ratio was estimated to be ~6:1 based on the relative fluorophore and protein absorbance ratio. However, such measurement was less reliable for labeled viruses due to the spectral overlap from a single RNA strand absorbance.

2.4. MS2 virus detection

To prepare for the detection of MS2 viruses, the porous silicon surfaces immobilized with unlabeled anti-MS2 antibodies were washed three times with 1 M NaCl in 0.02 M MES buffer solution. To minimize nonspecific binding, the surface was then blocked with 1 × PBS containing 1% (w/w) BSA and 0.05% (w/w) NaN₃ for 15 min under gentle mixing. After brief rinsing with deionized water, the surfaces were immersed in phosphate buffer (pH 7.0) (PBS), containing different concentrations of Alexa 532 dye-labeled MS2 viruses for 45 min. After that silicon surfaces were rinsed vigorously with PBS followed by water, and finally dried under a gentle stream of nitrogen gas.

2.5. Fluorescence measurement

The amounts of antibody and virus bound to the porous silicon surface were quantified by measuring the dye-labeled fluorescence intensity at the emission maximum (Fig. 2(b)). The emission spectra were recorded using a Fluorolog-3 spectrofluorimeter (Horiba Inc., Edison, NJ) equipped with a sample turret for the surface fluorescence measurements. The porous silicon wafers were mounted on microscope glass slides and placed in the sample compartment with the excitation beam incident at an angle of 60°. The background spectrum was recorded on PS samples that contained no fluorophores and was subtracted from the total signal. In all cases, an area near the center of the porous region was sampled. The observed fluorescence intensity was independent of the precise sample position, indicating the homogeneity and uniformity of the conjugated films.

3. Results and discussion

Before evaluating the sensor performance, it is important to quantify the degree of surface functionalization of the porous silicon films. One measurement that provides insight into the effectiveness of the surface functionalization techniques is to observe the wettability of the treated porous silicon, which is related to how well the antibody and analyte can infiltrate the porous matrix (Fan et al., 2004). We have performed such measurements on our PS surfaces using the sessile water drop contact angle technique. Fig. 2(a) plots the measured contact angle val-

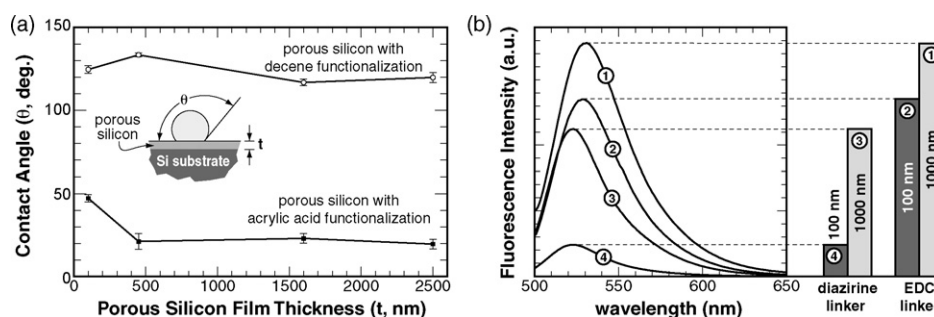


Fig. 2. (a) Contact angle of water on PS surfaces functionalized by decene/diazirine linker (open circles) and with acrylic acid/EDC linker (filled squares). (b) Fluorescence emission of the electrochemically etched porous silicon (PS) films with a covalently immobilized Alexa 488-labeled MS2 antibody, for two different film thicknesses and two different functionalization protocols: (1) 1000 nm PS film with EDC linker, (2) 100 nm PS film with EDC linker, (3) 1000 nm PS film with diazirine linker, and (4) 100 nm PS film with diazirine linker ($\lambda_{exc} = 488$ nm).

ues for surfaces treated with both decene and acrylic acid, for several porous layer thicknesses. It is clearly visible that methyl termination through photo-catalyzed reaction with decene provides a pronounced hydrophobic surface with an average contact angle around 130° for porous layer thicknesses up to $2.4 \mu\text{m}$. In contrast, the porous silicon surfaces functionalized with acrylic acid were distinctly hydrophilic, showing an average contact angle of 20° . The contact angle was observed to be independent of the film thickness for porous films that were thicker than 400 nm.

Optimal sensor performance is expected when the internal surface of the nanoporous silicon is completely covered with the capturing agent. Since the molecular size of the antibody is between 12 and 15 nm, we expect no mechanical barriers for its diffusion inside the porous layer with an average pore dimension of 50 nm (Fig. 1). However, direct observation of the antibody penetration proves difficult because of the small size of the antibody and the nanometer scale of the porous film. We therefore instead chose to measure the degree of fluorescence produced by conjugated porous silicon films with that were etched to different depths.

Dye fluorescence measurements were performed on porous silicon samples that were etched to 100 and 1000 nm thickness, and conjugated using both methods described above. Fig. 2(b) plots the measured fluorescence spectra for porous films conjugated using both the diazirine (decene) and EDC (acrylic acid) protocols. Both protocols show consistently higher fluorescence emission from the thicker porous layers, confirming that the Alexa 488-labeled antibody is penetrating the porous films. Furthermore, we observed no measurable fluorescence from bulk unetched silicon surfaces that were processed in parallel with the porous films.

The fluorescence intensity is not proportional to the film thickness, which suggests that the protein penetration could be less efficient in films that are thicker than 100 nm. This effect could also be caused by partial absorbance of excitation and emission photon flux by the underlying layers of the porous silicon film.

It is apparent that protein immobilization using EDC results in significantly higher film antibody content at both thickness

values (curves 1 and 2 in Fig. 2(b)) than the diazirine based conjugation (traces 3 and 4 in Fig. 2(b)). This effect can be explained on the basis of silicon surface hydrophobicity. The carboxyl termination used in the EDC protocol results in the hydrophilic surface (Fig. 2(a)), which facilitates efficient penetration of the aqueous protein solution inside the pore while the hydrophobic methyl termination, used in the diazirine protocol, results in significantly lower protein loading.

To test the efficacy of the porous silicon viral sensor, we exposed the antibody-conjugated films to solutions containing Alexa 532-labeled MS2 virus at several different concentrations. 100 nm thick PS films with antibodies immobilized by the EDC protocol were immersed for 45 min each in solutions containing the Alexa 532-labeled MS2 virus. The surface fluorescence was measured after thorough washing and drying. In these measurements, we used unlabeled antibodies to ensure that the entire received fluorescence signal originates from the captured MS2 virus. The relative amount of viral loading was gauged by measuring the fluorescence intensity of the exposed surface.

To confirm the role of the antibody in selectively capturing the MS2 virus, we exposed both conjugated and antibody-free films to the same solution containing labeled MS2 virus. As shown in Fig. 3(a), while the bio-conjugated film produces a significant fluorescence signal, we observe negligible fluorescence from the antibody-free porous silicon. This confirms that the covalently immobilized antibody inside of the porous film has selectively captured the antigen and that the washing and blocking procedure has effectively suppressed non-specific binding.

We tested the sensitivity and dynamic range of the sensor by exposing it to a series of solutions with viral concentrations ranging from 1×10^6 to 1×10^{12} plaque-forming units per mL (pfu/mL). Fig. 3(b) plots the fluorescence intensity as a function of viral concentration over this range. Based upon measurements of independently prepared samples, the error bars were estimated to be $\pm 25\%$ for all points, plus an uncorrelated absolute error of ± 300 (a.u.) representing the instrument resolution. We define the detection limit as the viral concentration at which the fluorescence signal is 3 standard deviations above the background level. From the data shown in Fig. 3(b), we obtain a detection

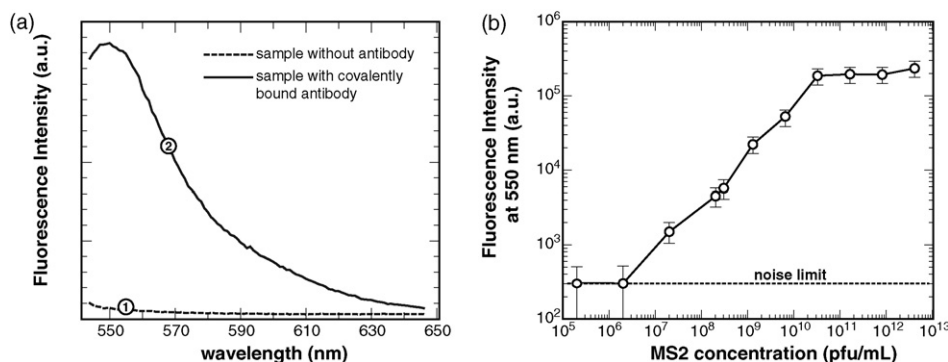


Fig. 3. (a) Fluorescence emission of the Alexa 532-labeled virus MS2, recorded on a porous silicon surface 100 nm thick, after 45 min exposure to solution containing 3.2×10^{10} pfu/mL virus MS2: (1) sample without antibody, (2) sample with covalently immobilized antibody ($\lambda_{\text{exc}} = 530$ nm). (b) Fluorescence emission of the Alexa 532-labeled virus MS2, recorded on a porous silicon surface 100 nm thick, after 45 min exposure to solution containing between 1×10^6 and 2×10^{12} pfu/mL virus MS2 ($\lambda_{\text{exc}} = 530$ nm).

limit of 2×10^7 pfu/mL, which compares favorably with the reported sensitivity of the MS2 micro-array (4.4×10^7 pfu/mL) and Luminex liquid array-based assays (3.5×10^6 pfu/mL) (Rao et al., 2004). The fluorescence intensity increases with viral concentration up to 2×10^{10} pfu/mL, above which the fluorescence signal saturates. Thus, the reported sensor allows measurement of viral concentrations ranging from 2×10^7 to 2×10^{10} (3 logs). For comparison, the Luminex dynamic range is from 1×10^6 to 1×10^9 pfu/mL (3 logs), and the micro-array dynamic range is 3×10^7 to 1×10^9 pfu/mL (1.5 logs).

4. Conclusions

A porous silicon surface provides a sensitive and robust platform for virus detection using immuno-capture. We have shown that a 100 nm thick porous layer with a covalently immobilized antibody has a sensitivity and dynamic range similar to that of the Luminex liquid array-based assay while clearly outperforming the protein micro-array device. It is expected that the sensor performance could be further improved by optimizing porous layer structure and thickness. Preliminary experiments have shown that the fluorescence yield increases with PS layer thickness up to a film thickness of about 400 nm, thus suggesting potentially lower detection limit and wider dynamic range. However, thicker films have also shown an intrinsic photoluminescence after conjugation procedures. This wide-band photoluminescence may interfere with antigen label fluorescence and raise the limit of detection. Our sensor platform could be easily adaptable for label-free detection based on index of refraction measurement where PS photoluminescence interferences can be ignored (Janshoff et al., 1998; Haake et al., 2000).

Acknowledgements

This work was supported by the UMD-NIST Center for Nanomanufacturing and Metrology (CNMM) and the Center for Nanoparticle Risk, Impact and Assessment (CNRIA).

References

- Bensliman, F., Mizuta, N., Matsumura, M., 2004. *J. Electroanal. Chem.* 568, 353–363.
- Borini, S., D'Auria, S., Rossi, M., Rossi, A.M., 2005. *Lab Chip* 5, 1048–1052.
- Buriak, J.M., 2002. *Chem. Rev.* 102, 1271–1308.
- Canham, L.T., 1990. *Appl. Phys. Lett.* 57, 1046–1048.
- Cullis, A.G., Canham, L.T., Calcott, P.D.J., 1997. *J. Appl. Phys.* 82, 909–965.
- DeStefano, L., Rendina, I., Moretti, L., Tundo, S., Rossi, A.M., 2004. *Appl. Opt.* 43, 167–172.
- Fan, J.G., Tang, X.J., Zhao, Y.P., 2004. *Nanotechnology* 15, 501–504.
- Föll, H., 1991. *Appl. Phys. A* 53, 8–19.
- Haake, H.M., Schütz, A., Gauglitz, G., 2000. *Fresen. J. Anal. Chem.* 366, 576–585.
- Herino, R., Bomchil, G., Barla, K., Bertrand, C., Ginoux, J.L., 1987. *J. Electrochem. Soc.* 134, 1994–2000.
- Janshoff, A., Dancil, K.P.S., Steinem, C., Greiner, D.P., Lin, V.S.Y., Gurtner, C., Motesharei, K., Sailor, M.J., Ghadiri, M.R., 1998. *J. Am. Chem. Soc.* 120, 12108–12116.
- Mathew, F.P., Alocilja, E.C., 2005. *Biosens. Bioelectron.* 20, 1656–1661.
- Rao, R.S., Visuri, S.R., McBride, M.T., Albala, J.S., Matthews, D.L., Coleman, M.A., 2004. *J. Prot. Res.* 3, 736–742.
- Stockley, P.G., Stonehouse, N.J., Valegard, K., 1994. *Int. J. Biochem.* 26, 1249–1260.
- Uhlir, A., 1956. *Bell Syst. Technol. J.* 35, 333–347.
- Wang, L., Reipa, V., Blasic, J., 2004. *Bioconjugate Chem.* 15, 409–412.
- Wick, C.H., McCubbin, P.E., 1999. *Toxicol. Meth.* 9, 245–252.